Supporting material for:
Flow dynamics through discontinuous clogs of rigid particles in tapered microchannels

Olukayode T. Majekodunmi[1] **and Sara M. Hashmi**[1,2,3,*]

[1]Department of Chemical Engineering, Northeastern University, Boston, MA 02115
[2]Department of Mechanical and Industrial Engineering, Northeastern University, Boston, MA 02115
[3]Department of Chemistry and Chemical Biology, Northeastern University, Boston, MA 02115
[*]s.hashmi@northeastern.edu

Hydraulic Resistance of the Microfluidic Device

The hydraulic resistance, R_H, was estimated by flowing pure water through each microfluidic device at driving pressures, ΔP, in the range 0 – 2000 mbar. This was done after the device had first been filled with pure water. ΔP was increased stepwise and the respective flowrates were recorded. As illustrated in Fig. S1, the results were fitted to Hagen-Poiseuille's law for pressure-driven flow in a cylindrical pipe which is simplified as $Q = \Delta P / R_H$.

R_H is constant for any device, provided the geometric parameters and fluid conditions are the same. The mean R_H of the devices used in this study was estimated to be $\sim$80 mbar·min·μL^{-1} with a standard deviation of $\sim$5 mbar·min·μL^{-1} (see Table S1 for the respective values of each device). Also, the devices were not deforming to allow more flow under high ΔP as demonstrated by the linearity of the Q *vs.* ΔP plots over the range of ΔP explored in this study.

By considering the inlet reservoir and channels region of the microfluidic device as two fluidic resistors in series, the greatest hydraulic resistance appears to be in the channel region as the R_H of the device (inlet reservoir and channel region combined) is, at least, an order of magnitude more than that of the inlet reservoir (Fig. S1).

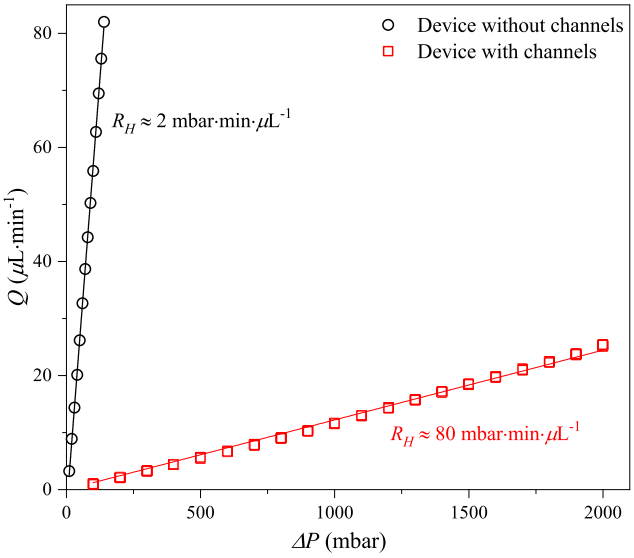

Figure S1. Linear ramp of ΔP with pure water to estimate R_H of the microfluidic device (inlet reservoir and channels combined) and inlet reservoir (device without channels).

Number of Clogging Events

Fig. S2 shows the number of clogging events, N, varies linearly as ϕ for constant ΔP. Also, it suggests there is a minimum number of clogs required for the device to be "fully clogged" - which is $\sim$750 in this case. By extension, it implies a minimum

number of particles is also required for the device to be "fully clogged."

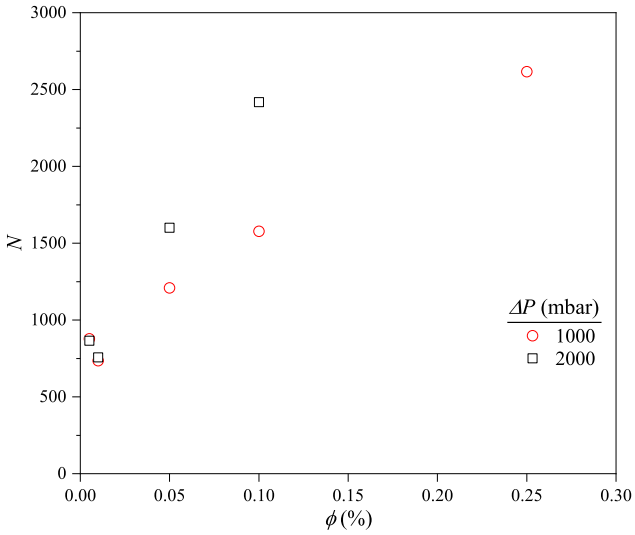

Figure S2. Number of clogging events vary linearly as ϕ for flow tests conducted at ΔP.

Suspension Flowrate Decay

Presented in Fig. S3 is the flowrate decay curves at different ΔP when $\phi = 0.01$ and 0.10%. It shows the flowrate decay is faster at $\phi = 0.10\%$ for each ΔP. Also, each decay curve features three distinct timescales: a power-law flowrate decay preceded by an initial plateau which ends at $t = \tau_d$, and succeeded by a final plateau or slower decay rate depending on ϕ. A final plateau is reached at $t \equiv \tau_f \approx 400$ s when $\phi = 0.10\%$. It signifies the end of the flowrate decay. However, a final plateau is not observed at $\phi = 0.01\%$: instead, the cake continued to grow but at a much slower rate.

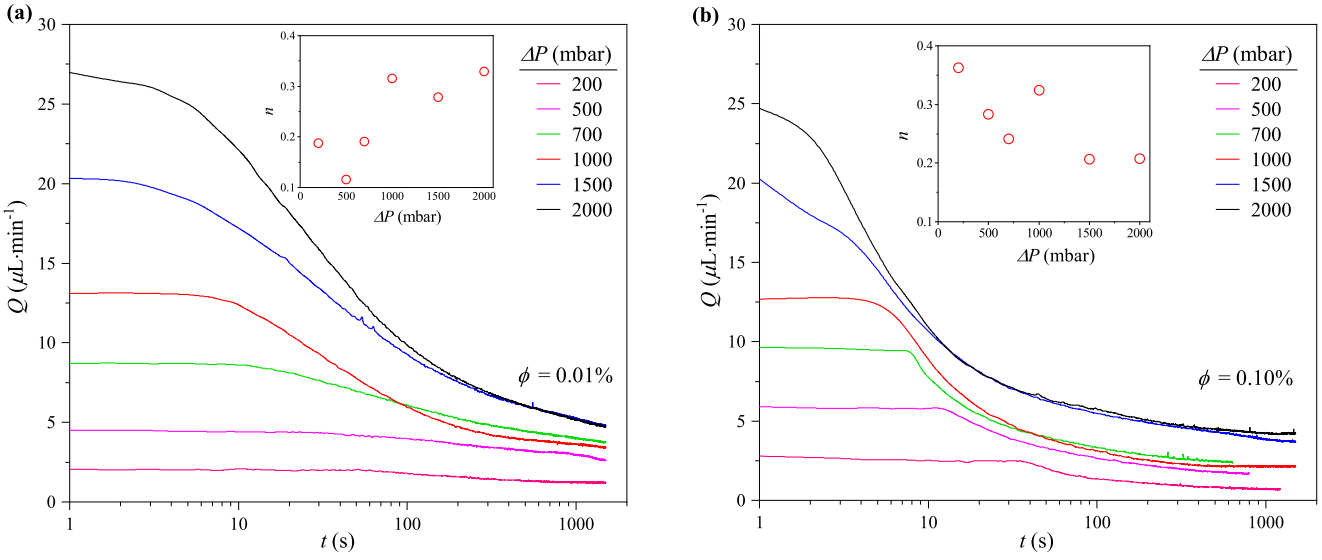

Figure S3. Suspension flowrate decays at different ΔP for: (a) $\phi = 0.01\%$, and (b) 0.10%. Inset: Exponents, n, of the power-law decays ($Q \backsim t^{-n}$) plotted as a function of ΔP. The value of n slightly increased with increasing ΔP when $\phi = 0.01\%$, and decreased when $\phi = 0.10\%$.

Evolution of Fluorescence Intensity

Changes in the intensity of fluorescence signals (I/I_m) at the midpoint of the channel exit area were analyzed for some flow tests to estimate the end of the initial plateau (τ_d) in the flowrate decay curves. The result when ΔP = 2000 mbar and ϕ = 0.05% is presented in Fig. S4. It indicates significant increases in I/I_m in the first second of the flow test, which is less than the time it takes to fill the device with pure water ($\tau_v = V_d/Q$) at the same ΔP: $\tau_v = V_d R_H/\Delta P$, where V_d is the total volume of the device calculated to be $\sim$2 μL. In this case, $\tau_v \approx 5$ s while $\tau_d \approx 1$ s.

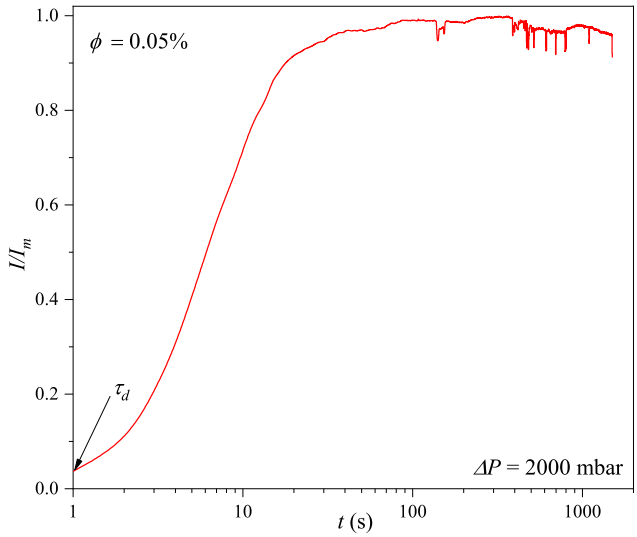

Figure S4. Evolution of fluorescence intensity (I/I_m) at the midpoint of the channels exit, when ΔP = 2000 mbar and ϕ = 0.05%.

Decay Timescales and Power-law Exponents

The timescales and exponents of the power-law fits observed both when the decay curve reaches a final plateau and otherwise are presented in Table S1 for all conditions of ΔP and ϕ examined in this study.

Table S1. Hydraulic resistances, timescales and exponents of the power-law decays, and post-clogging Darcy permeability of the microfluidic devices.

					n[a]	
	ϕ (%)	R_H (mbar·min·μL^{-1})	τ_d (s)	τ_f (s)	Rapid decay[b]	Slow decay[c]
	0.005	78.13	11	400 – 600	0.28	0.16
	0.01	76.92	10	400 – 600	0.32	0.13
ΔP = 1000 mbar	0.05	80.00	6	500	0.33	-
	0.10	78.13	5	500	0.32	-
	0.25	70.42	4	500	0.27	-

					n		
	ΔP (mbar)	R_H (mbar·min·μL^{-1})	τ_d (s)	τ_f (s)	Rapid decay	Slow decay	κ (μm^2)
	200	89.29	60	400 – 600	0.19	0.15	
	500	107.53	17	400 – 600	0.12	0.14	0.60
	700	78.74	13	400 – 600	0.19	0.17	
ϕ = 0.01%	1000	76.92	10	400 – 600	0.32	0.13	
	1500	78.74	2	400 – 600	0.28	0.20	0.32
	2000	81.97	1	400 – 600	0.33	0.23	

					n		
	ΔP (mbar)	R_H (mbar·min·μL^{-1})	τ_d (s)	τ_f (s)	Rapid decay	Slow decay	κ (μm^2)
	200	84.03	52	500	0.37	-	
	500	82.64	17	500	0.25	-	0.46
	700	90.09	13	500	0.27	-	
ϕ = 0.05%	1000	80.00	6	500	0.33	-	
	1500	81.30	2	400 – 600	0.26	0.14	0.27
	2000	78.74	1	400 – 600	0.23	0.15	

					n		
	ΔP (mbar)	R_H (mbar·min·μL^{-1})	τ_d (s)	τ_f (s)	Rapid decay	Slow decay	κ (μm^2)
	200	72.46	40	600	0.36	-	
	500	81.30	12	600	0.28	-	0.40
	700	71.43	8	600	0.24	-	
ϕ = 0.10%	1000	78.13	5	500	0.32	-	
	1500	78.74	2	600	0.21	-	0.26
	2000	79.37	1	600	0.21	-	

[a] The power-law exponent in $Q \backsim t^{-n}$.

[b] The power-law exponent, n, corresponding to the clog growth timescale.

[c] The power-law exponent, n, associated with the point of inflection on the decay curve when a final plateau was not reached. If a plateau is reached beyond τ_f, '-' is shown in lieu of a value for n.